

Disorder Induced Ferromagnetism in CaRuO_3

T. He and R.J. Cava

Department of Chemistry and Princeton Materials Institute, Princeton University

Princeton, New Jersey 08540, U.S.A.

(Received 23 November, 2000)

Abstract

The magnetic ground state of perovskite structure CaRuO_3 has been enigmatic for decades. Here we show that paramagnetic CaRuO_3 can be made ferromagnetic by very small amounts of partial substitution of Ru by Ti. Magnetic hysteresis loops are observed at 5 K for as little as 2% Ti substitution. Ti is non-magnetic and isovalent with Ru, indicating that the primary effect of the substitution is the disruption of the magnetic ground state of CaRuO_3 through disorder. The data suggest that CaRuO_3 is poised at a critical point between ferromagnetic and paramagnetic ground states.

I. INTRODUCTION

The ruthenate perovskites and their layered variants provide an important testing ground for current ideas in the magnetism of complex systems, and in particular, the possible relationships between magnetism and superconductivity.¹⁻⁹ The changes from ferromagnetism to superconductivity on going from three-dimensional SrRuO_3 to two-dimensional Sr_2RuO_4 ,¹⁻⁴ and from ferromagnetism to paramagnetism on going from SrRuO_3 to CaRuO_3 ¹⁰⁻¹³ are important cornerstones for defining the fundamental character of the whole family. CaRuO_3 , cited in past discussions as a paramagnetic material with antiferromagnetic spin interactions, establishing a baseline for “normal” magnetic behavior in this system, is in actuality quite problematic. Recently, a new context for understanding CaRuO_3 has been proposed, in which CaRuO_3 is considered to be a nearly ferromagnetic metal, rather than a classical Curie-Weiss antiferromagnet.¹⁴⁻¹⁷ Here we show that small amounts of disorder introduced into CaRuO_3 by partial substitution of Ru by non-magnetic, isovalent Ti (Ti^{4+} has electron configuration $3d^0$) induce clear ferromagnetic behavior at low temperatures: magnetic hysteresis loops are observed at 5 K for as little as 2% Ti substitution. CaRuO_3 itself appears to show magnetic behavior which is part of a continuous trend towards increasing ferromagnetism induced by increasing disorder, and thus appears to be poised at a critical point between ferromagnetism and paramagnetism at low temperatures.

II. EXPERIMENTAL

Samples of $\text{CaRu}_{1-x}\text{Ti}_x\text{O}_3$ ($0 \leq x \leq 1$) were prepared by conventional solid state reaction using CaCO_3 (99.8% Mallinckrodt), dried RuO_2 (99.95% Cerac) and TiO_2 (99.9+% Alfa). The starting materials were mixed in stoichiometric proportion, and heated in dense Al_2O_3 crucibles at 1000°C in air for three days with intermediate grindings. About 5% wt. KCl was added to the samples as a reaction rate enhancer. The powders were then pressed into

pellets and heated in dense Al_2O_3 boats at 1250°C in air for two days with intermediate grindings. Samples were investigated by powder X-ray diffraction with $\text{Cu K}\alpha$ radiation at room temperature; a small amount of fine tungsten powder was mixed with each ground sample as an internal standard. The cell parameters were refined by least squares fitting of powder X-ray diffraction reflection positions.

Electrical resistivity was measured in the range of 5-300 K using a standard four-lead AC technique on polycrystalline sample bars about $1 \times 1 \times 5 \text{ mm}^3$ in size. The magnetic properties were studied in a Quantum Design PPMS system. Magnetic susceptibility data were collected in the temperature range 5-300 K in a DC field of 1 Tesla on field cooling. The magnetic hysteresis loops were taken in 5 or 10 K steps between 5 K and 55 K for each sample, in a magnetic field ranging from -2 to 2 Tesla.

III. RESULTS AND DISCUSSION

The X-ray patterns show that all samples of $\text{CaRu}_{1-x}\text{Ti}_x\text{O}_3$ ($0 \leq x \leq 1$) have the GdFeO_3 -type orthorhombic perovskite structure with no secondary phases detected. The refined cell parameters are shown in the main panel of Fig. 1: a and b decrease, while c increases smoothly when Ru^{4+} (0.62 \AA) is substituted by smaller Ti^{4+} (0.605 \AA). The inset to Fig. 1 gives the temperature dependence of the resistivity for selected compositions of polycrystalline samples of $\text{CaRu}_{1-x}\text{Ti}_x\text{O}_3$. CaRuO_3 is metallic, while the resistivity of $\text{CaRu}_{1-x}\text{Ti}_x\text{O}_3$ goes up systematically on Ti-doping. The grain boundary resistance has a significant effect on the observed resistivity, so no quantitative conclusions can be drawn from the data. However the observed transition from metallic CaRuO_3 to insulating CaTiO_3 is as expected, as Ti^{4+} has no d electrons and Ti-O hybridization is poor.

The temperature dependence of inverse magnetic susceptibility measured at 1 T on field cooling is shown in Fig. 2. The inverse magnetic susceptibility decreases

systematically when x goes from 0 to 0.4, with slightly increasing slopes in the high temperature region. When x is greater than 0.4, however, $1/\chi$ begins to increase as shown in the inset of Fig. 2. (CaTiO₃ is diamagnetic and is excluded from the figure.) The high temperature data can be well described by fitting to the Curie-Weiss law. All samples, however, including CaRuO₃ itself, show a systematic S-shaped downward trend below 50 K. Similar behavior has been observed in Sr doped CaRuO₃, and was attributed to the occurrence of Sr clusters in the solid solution, leading to short-range ordered ferromagnetic regions of SrRuO₃.¹⁸ There are no Sr ions present in the current system. The same type of short-range ferromagnetic behavior has therefore been introduced in CaRuO₃ by Ti doping.

The Curie-Weiss temperature, θ_{CW} , derived by fitting the 150-300 K data in Fig. 2 to the Curie-Weiss law, is shown as a function of composition in Fig. 3. A temperature independent term, χ_0 , is included in the fits and determined to a precision of $\pm 5 \times 10^{-5}$ emu/mol Ru. The substitution of Ti for Ru systematically shifts θ_{CW} towards positive values for $x \leq 0.4$, changing from $\theta_{CW} = -162$ K for $x=0$ to $\theta_{CW} = -37$ K for $x=0.4$. The composition dependence of the effective magnetic moment, μ_{eff} , also derived from the data in Fig. 2, is shown in the inset of Fig. 3. The μ_{eff} per mole CaRu_{1-x}Ti_xO₃ formula unit decreases smoothly with increasing Ti content, as expected from the non-magnetic nature of Ti⁴⁺. The μ_{eff} per mole Ru, however, stays constant across the series, at approximately $2.8 \mu_B/\text{Ru}$, corresponding to the value expected for a low spin Ru⁴⁺ ($S=1$) configuration. This result is in accord with the fact that CaRu_{1-x}Ti_xO₃ is an isovalent doping series. The Ru atom still has a valence of 4+ and it is still in an octahedral site. The only change is that the long-range three-dimensional Ru-O-Ru network in CaRuO₃ is disrupted by disorder, as the B-site is occupied both by conducting and magnetic Ru⁴⁺ and by insulating and nonmagnetic Ti⁴⁺.

The disorder introduced in B sites has a significant yet unexpected effect on the magnetic properties. Though the meaning of the Curie-Weiss temperature in a complex magnetic system such as this is not clear, it can be considered as an order parameter for characterizing the progression between classical ferromagnetic and non-ferromagnetic behavior.¹⁸ There is a clear trend towards increasing ferromagnetism on Ti-doping, as can be seen by the more positive Curie-Weiss temperatures. This trend is further confirmed by the magnetization measurements. The main panel of Fig. 4 shows the magnetic hysteresis loops measured for a variety of CaRu_{1-x}Ti_xO₃ compositions at 5 K, and the lower left inset shows the data for $x=0.02$. It is remarkable that as little as 2% Ti substitution creates a hysteresis loop, which indicates that the magnetic ground state has a significant ferromagnetic component. There are no other sources of possible ferromagnetism, i.e., all possible impurities like CaRuO₃, CaTiO₃, TiO₂, RuO₂ or Ca₃Ru₂O₇, are not ferromagnets. This ferromagnetism is therefore an intrinsic property of the compound. The sizes of the loops increase until x equals 0.4, and then decrease as the

samples approach the non-magnetic end member CaTiO₃. It is important to note that the change in cell dimension and distortion of CaRuO₃ on Ti doping (inset to Fig. 1) is opposite to the effect observed in the Ca_{1-x}Sr_xRuO₃ series.¹⁹ Therefore the induced ferromagnetism cannot be explained by the arguments often employed to explain the difference between "paramagnetic" CaRuO₃ and ferromagnetic SrRuO₃.¹⁰⁻¹² We note that unlike in the present case, where ferromagnetism has been induced in CaRuO₃ by doping with non-magnetic Ti, no ferromagnetism was reported in the CaRu_{1-x}Sn_xO₃ series,²⁰ probably due to a very large disruption of the Ru-O sublattice by chemically and metrically dissimilar Sn. The substitution of Rh in CaRuO₃ has been reported,²¹ but Rh is expected to change both the oxidation state of Ru and to have a magnetic contribution as well.

The magnetization was measured as a function of magnetic field (M - H curve) in the temperature range 5-55 K for each sample. All M - H plots show straight lines between 1 T and 2 T. At each temperature, the ferromagnetic contribution to the magnetization, M_F , was obtained by extrapolating the magnetization at higher field to zero field. The inset in the upper left panel of Fig. 4 shows M_F as a function of temperature for $x=0.2, 0.4, 0.6,$ and 0.8 . For each sample, the sizes of the hysteresis loop decrease with increasing temperature, as reflected in the decreasing M_F . The temperature at which ferromagnetism turns on is, within our precision, independent of the Ti doping content, i.e., all loops are closed at 55 K, and a hysteresis loop can be observed only at lower temperature. Therefore the ferromagnetic T_C is 55 K and independent of composition from $x=0.2$ to $x=0.8$. The magnitude of the largest M_F/Ru , ~ 530 emu/mol Ru at 5 K for $x=0.4$, is considerably lower than that observed for SrRuO₃, which is in the range of ~ 4700 - 8900 emu/mol Ru.²² These magnetizations are consistent with an itinerant electron picture of ferromagnetism in both materials.¹⁴⁻¹⁶ Preliminary neutron diffraction experiments at 13 K on CaRu_{0.5}Ti_{0.5}O₃ showed that there are no additional magnetic neutron scattering peaks, indicating that these materials are not canted antiferromagnets.²³

IV. CONCLUSION

The magnetic ground state of CaRuO₃ is problematic. Once thought to be a conventional paramagnetic metal with antiferromagnetic spin interactions, it has recently been proposed to be a nearly ferromagnetic metal, for which a classical Curie-Weiss type interpretation of the magnetic susceptibility is not valid. In the current study, samples of CaRu_{1-x}Ti_xO₃ ($0 \leq x \leq 1$) were prepared and studies of their magnetic properties show that CaRuO₃ can be made to display ferromagnetic behavior by introducing very small amounts of disorder onto the Ru sites by partial substitution of Ru by non-magnetic, isovalent Ti. All Ti-doped samples show magnetic hysteresis loops below 55 K and the substitution systematically shifts the Curie-Weiss

temperatures towards positive values. The disorder induced ferromagnetism cannot be explained in a conventional band-structure based picture, as the disorder would be expected to decrease the density of states at the Fermi level, favoring a non-magnetic ground state.¹¹⁻¹² Rather the data imply that CaRuO₃ itself is poised at a critical point between ferromagnetism and paramagnetism at low temperatures, a balance tipped in favor of the former by small amounts of disorder. This strongly supports the proposal that the magnetic ground state of CaRuO₃ is that of a nearly ferromagnetic metal, not a classical antiferromagnet. Thus, conventional magnetic behavior in the family of perovskite-based ruthenates remains elusive.

ACKNOWLEDGMENTS

This work was supported by the National Science Foundation grant No. DMR-9725979.

Reference:

- ¹ A. Callaghan, C.W. Moeller, and R. Ward, *Inorg. Chem.* **5**, 1572 (1966).
- ² D. J. Singh, *J. Appl. Phys.* **79**(8), 4818 (1996).
- ³ Y. Maeno, H. Hashimoto, K. Yoshida, S. Nishizaki, T. Fujita, J. G. Bednorz and F. Lichtenberg, *Nature* **372**, 532 (1994).
- ⁴ I.I. Mazin and D.J. Singh, *Phys. Rev. Lett.* **79**, 733 (1997).
- ⁵ I.I. Mazin and D.J. Singh, *Phys. Rev. Lett.* **82**, 4324 (1999).
- ⁶ S. Nakatsuji, S.-I. Ikeda and Y. Maeno, *J. Phys. Soc. Jpn.* **66**(7), 1868 (1997).
- ⁷ R. J. Cava, H. W. Zandbergen, J. J. Krajewski, W. F. Peck, Jr., B. Batlogg, S. Carter, R. M. Flemming, O. Zhou, and L. W. Rupp, Jr., *J. Solid State Chem.* **116**, 141 (1995).
- ⁸ S.-I. Ikeda and Y. Maeno, *Physica B.* **261**, 947 (1999).
- ⁹ I.I. Mazin and D.J. Singh, *J. Phys. Chem. Solids* **59**, 2185 (1998).
- ¹⁰ F. Fukunaga and N. Tsuda, *J. Phys. Soc. Jpn.* **63**, 3798 (1994).
- ¹¹ I.I. Mazin and D. J. Singh, *Phys. Rev. B* **56**(5), 2556 (1997).
- ¹² G. Santi and T. Jarlborg, *J. Phys.: Condens. Matter* **9**, 9563 (1997).
- ¹³ G. Cao, S. McCall, M. Shepard, and J.E. Crow, *Phys. Rev. B* **56**, 321 (1997).
- ¹⁴ K. Yoshimura, T. Imai, T. Kiyama, K. R. Thurber, A. W. Hunt, and K. Kosuge, *Phys. Rev. Lett.* **83**(21), 4397 (1999).
- ¹⁵ T. Kiyama, K. Yoshimura, K. Kosuge, H. Michor and G. Hilscher, *J. Phys. Soc. Jpn.* **67**, 307 (1998).
- ¹⁶ T. Kiyama, K. Yoshimura and K. Kosuge, *J. Phys. Soc. Jpn.* **68**, 3372 (1999).
- ¹⁷ H. Mukuda, K. Ishida, Y. Kitaoka, K. Asayama, R. Kanno and M. Takano, *Phys. Rev. B* **60**, 12279 (1999).
- ¹⁸ T. He, Q. Huang and R.J. Cava, accepted by *Phys. Rev. B*.
- ¹⁹ H. Kobayashi, M. Nagata, R. Kanno and Y. Kawamoto, *Mater. Res. Bull.* **29**, 1271 (1994).
- ²⁰ G. Cao, S. McCall, J. Bolivar, M. Shepard, F. Freibert, P. Henning, and J.E. Crow, *Phys. Rev. B* **54**, 15144 (1996).
- ²¹ G. Cao, F. Freibert, and J.E. Crow, *J. Appl. Phys.* **81**, 3884 (1997).
- ²² J.M. Longo, P.M. Raccach and J.B. Goodenough, *J. Appl. Phys.* **39**, 1327 (1968).
- ²³ Q. Huang, J. Lynn, T. He, and R.J. Cava, unpublished data.

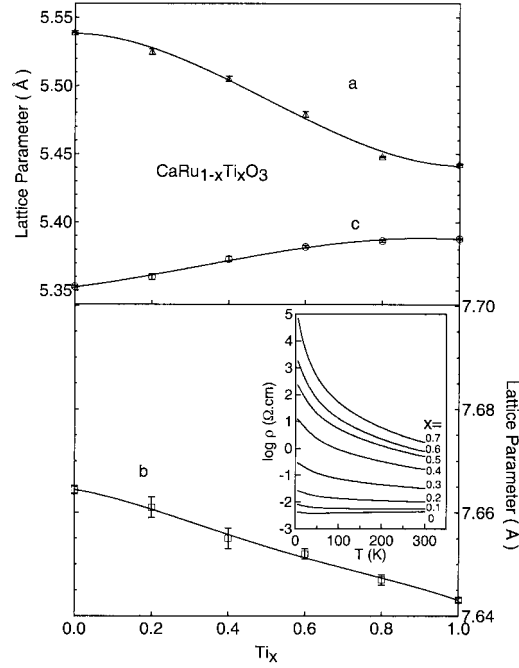


FIG. 1. Unit cell dimensions for orthorhombic $\text{CaRu}_{1-x}\text{Ti}_x\text{RuO}_3$ as a function of Ti doping content, solid lines are guides to the eye. Inset: Temperature dependence of the electrical resistivity of polycrystalline samples of $\text{CaRu}_{1-x}\text{Ti}_x\text{RuO}_3$.

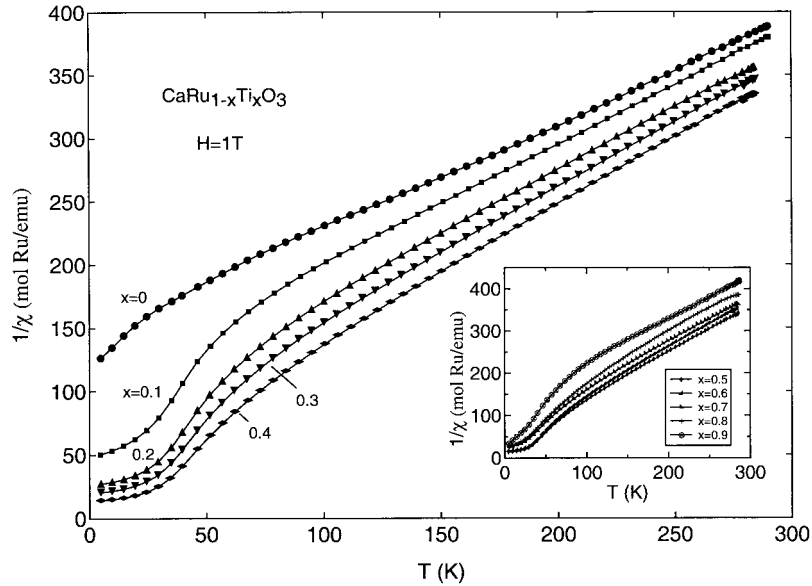


FIG. 2. Temperature dependence of the inverse magnetic susceptibility measured at 1 T on field cooling for $\text{CaRu}_{1-x}\text{Ti}_x\text{RuO}_3$ ($0 \leq x \leq 0.4$). Inset: same data for $0.4 \leq x \leq 0.9$.

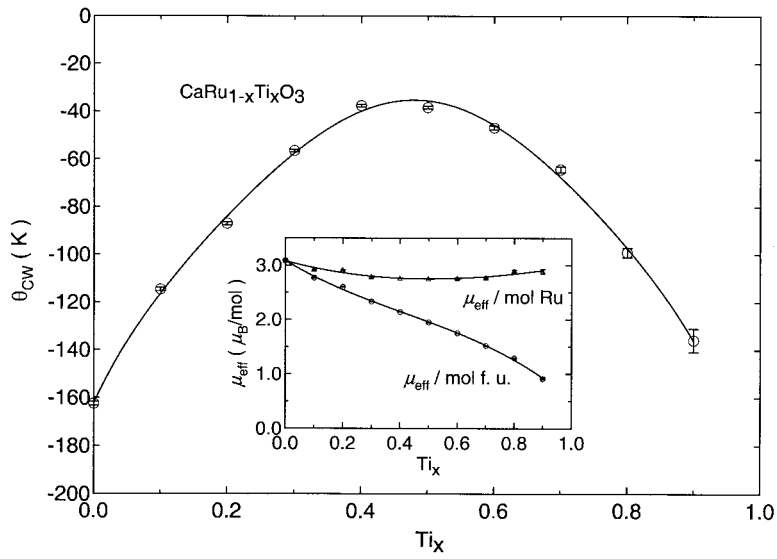


FIG. 3. Composition dependence of Curie-Weiss temperatures for $CaRu_{1-x}Ti_xRuO_3$. Inset: Composition dependence of the effective magnetic moment calculated in per mole formula unit (\circ) and in per mole Ru (Δ). Solid lines are guides to the eye.

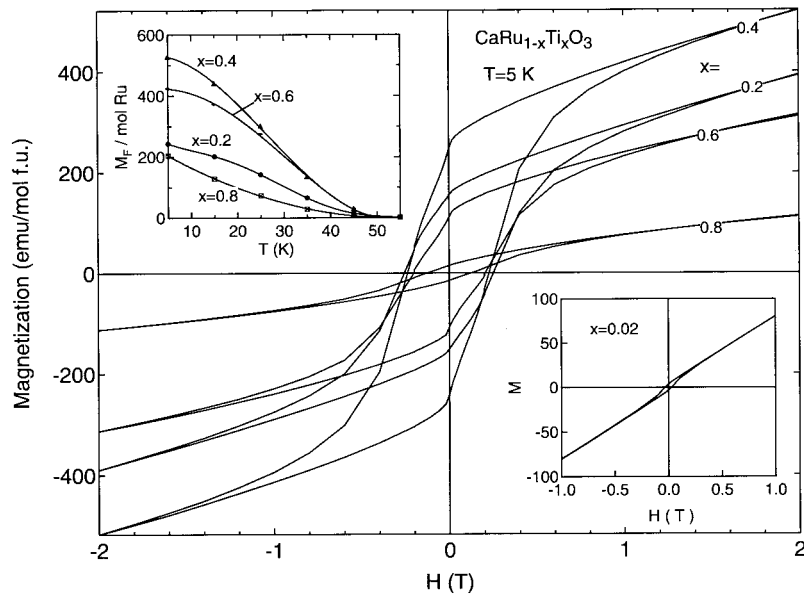


FIG. 4. Magnetic hysteresis loops for $CaRu_{1-x}Ti_xRuO_3$ at 5 K for $x=0.2, 0.4, 0.6$ and 0.8 . Inset, upper left: Temperature dependence of the ferromagnetic contribution to magnetization for $CaRu_{1-x}Ti_xRuO_3$ with $x=0.2, 0.4, 0.6$ and 0.8 . Inset, lower right: Magnetic hysteresis loop for $CaRu_{0.98}Ti_{0.02}RuO_3$ at 5 K.